Alma Mater Studiorum Università di Bologna
Archivio istituzionale della ricerca

Ab Initio Study of Polytetrafluoroethylene Defluorination for Tribocharging Applications

20 April 2024

Ab Initio Study of Polytetrafluoroethylene Defluorination and its Possible Effects on Tribocharging

Giulio Fatti,*,† Maria Clelia Righi,‡ Daniele Dini,¶ and Alessandra Ciniero¶

†*Department of Physics, Informatics and Mathematics, University of Modena and Reggio Emilia, Modena*

‡*Department of Physics and Astronomy, University of Bologna, Italy*

¶*Department of Mechanical Engineering, Imperial College London*

E-mail: giulio.fatti@unimore.it

Abstract

Polytetrafluoroetyhlene (PTFE) is one of the most efficient polymers for green energy-harvesting devices like triboelectric nanogenerators because of its high capability of acquiring and retaining negative charge. Despite its extensive use, the relation between PTFE triboelectric behavior and its electronic properties has never been analyzed. To shed light on this important feature we have studied the electronic properties of PTFE low-index surfaces in the high pressure phase by means of density functional theory. We start by showing that adding either a positive or a negative charge on pristine surfaces is energetically unfavorable. We then demonstrate the role played by surface defects. When a surface fluorine vacancy is introduced the analysis of the band structure reveals that the defect generates a trap state that enables the surface to acquire and retain negative charge.

1

Introduction

Polytetrafluoroethylene (PTFE) is one of the most used insulating polymers for many technological applications that require specific frictional, electrical, and chemical properties. In particular, PTFE is widely used for technologies based on triboelectrification, such as the triboelectric nanogenerators (TENGs)[1–4]. These are green energy-harvesting devices that can convert mechanical energy into electricity at zero emissions by coupling triboelectrification and electrostatic induction.

Triboelectrification refers to the contact-induced electrification effect that occurs when a material is put in contact and/or rubbed against a different material. Despite being one of the most known and long studied physical phenomena, triboelectrification is still poorly understood[5,6] and the mechanism behind it is still under debate especially for insulator-insulator contact. Several theories have suggested that the electrification is due to the transfer of electrons[7–13], ions[14–17] or microscopic fragments of material[18–21] that act as charge carriers, however, no consensus has been yet achieved.

This lack of fundamental understanding of triboelectrification hinders the development and the improvement of effective TENGs. So far, a triboelectric series has been used to determine the relative tribopolarity between two materials. The order indicates the direction of charge transfer when two different materials are rubbed against each other; the material high in the series charges positively when paired with a material at lower position and *vice versa.*[22,23]

It has been known for nearly a decade that the net charging corresponds to a little imbalance between the charges, both negative and positive, transferred between the surfaces in both directions, resulting in a mosaic charge pattern.[20,24] Despite this fact, PTFE is characterized by a high capability of acquiring and retaining a net negative charge, reason why it is one of the most used materials for TENGs technologies. In fact, the mosaic pattern and the positive charges found on PTFE surfaces have been attributed to material transfer from the other material in contact across the interface.[20] PTFE can be found indeed at the

lowest position in many triboelectric series.[22,23]

Despite the fact that several experimental[25–29] and theoretical[30–33] studies on the electronic properties of PTFE have been conducted, no one of them analyzed the relation between its triboelectric behavior and electronic properties, specifically in the high pressure phase. This phase is known to be stable over 0.65 GPa[34–36] and it is the most occurring in tribological conditions, in fact the pressure at the microscopic scale can easily exceed 5 GPa[37].

Previous theoretical studies on polyethylene (PE), located as well at the bottom of the triboelectric series, discovered that the presence of PE surfaces can lead to the formation of surface states inside the band gap, independently of the surface orientation.[38] These states, located under the conduction band, act as deep traps for electrons, making PE a suitable electron attractor. This is particularly interesting because PE is just above PTFE in the triboelectric series and it has the same lattice structure as PTFE, thus a similar behavior is expected.

Here we present, for the first time, insights into the relation between the triboelectric behavior of PTFE low-index surfaces in the high pressure phase and their electronic properties, by employing an *ab-initio* approach. To start with, we studied the structural and electronic properties of low-index surfaces, PTFE(100), PTFE(010) and PTFE(110). Then, in order to verify the formation of electron trap states on the surface we introduced, alternatively, a positive and a negative charge and we evaluated their localization. Finally, we investigated the influence of a surface fluorine vacancy on the electronic properties and we demonstrated that the presence of defects is key for the PTFE capability of acquiring and retaining negative charge.

Computational Methods

We studied the structural and electronic properties of the high-pressure PTFE low-index surfaces by means of density functional theory (DFT) calculations as implemented in the Quantum ESPRESSO (QE) package[39]. The exchange-correlation functional is described by the general gradient approximation (GGA) in the Perdew-Burke-Ernzerhof (PBE) parametrization[40] corrected by a dispersion term (PBE-D) to model the long-range inter-chain van der Waals (vdW) interactions. The dispersion term was introduced using the semi-empirical Grimme method[41]. The scaling parameter of the Grimme correction was tuned to a value of 0.42 to reproduce a cohesive energy density consistent with the experimental values.[42] The ionic species are described by ultrasoft pseudopotentials (PP's). A kinetic energy cutoff of 40 Ry (320 Ry) was chosen to truncate the expansion of the wave functions (charge density). The chosen lattice parameters $a = 8.70$ Å, $b = 5.97$ Å, with a setting angle $\alpha = 37/38°$, were obtained in our previous study on the bulk properties of PTFE[42], and they are in good agreement with the experimental values $a_{exp} = 8.73$ Å[26], $b_{exp} = 5.69$ Å[26], and $\alpha_{exp} = 35°$[34].

To model the low-index PTFE(100) and PTFE(010) surfaces a (2×2) supercell (Fig. 1a,b) were considered and a vacuum region of 25 Å were added to separate the periodic replicas. The PTFE(110) surface is modeled by a (1×2) orthorhombic supercell with the vacuum region of the same thickness of PTFE(100) and PTFE(010) surfaces. In this way the three modelled surfaces all have the same number of atoms, 192, distributed in 4 layers. A $2\times2\times1$ Monkhorst-Pack grid[43] was used to sample the Brillouin zone of the supercells.

The defective surface was realized by removing one fluorine atom from one of the PTFE chains at the surface. Spin polarized DFT was used to describe correctly the uncoupled electron caused by the removal of a C-F bond and a Gaussian broadening was used for the calculation of fractional occupancies, with a smearing width of 0.005 Ry.

The planar averaged charge density was calculated as:

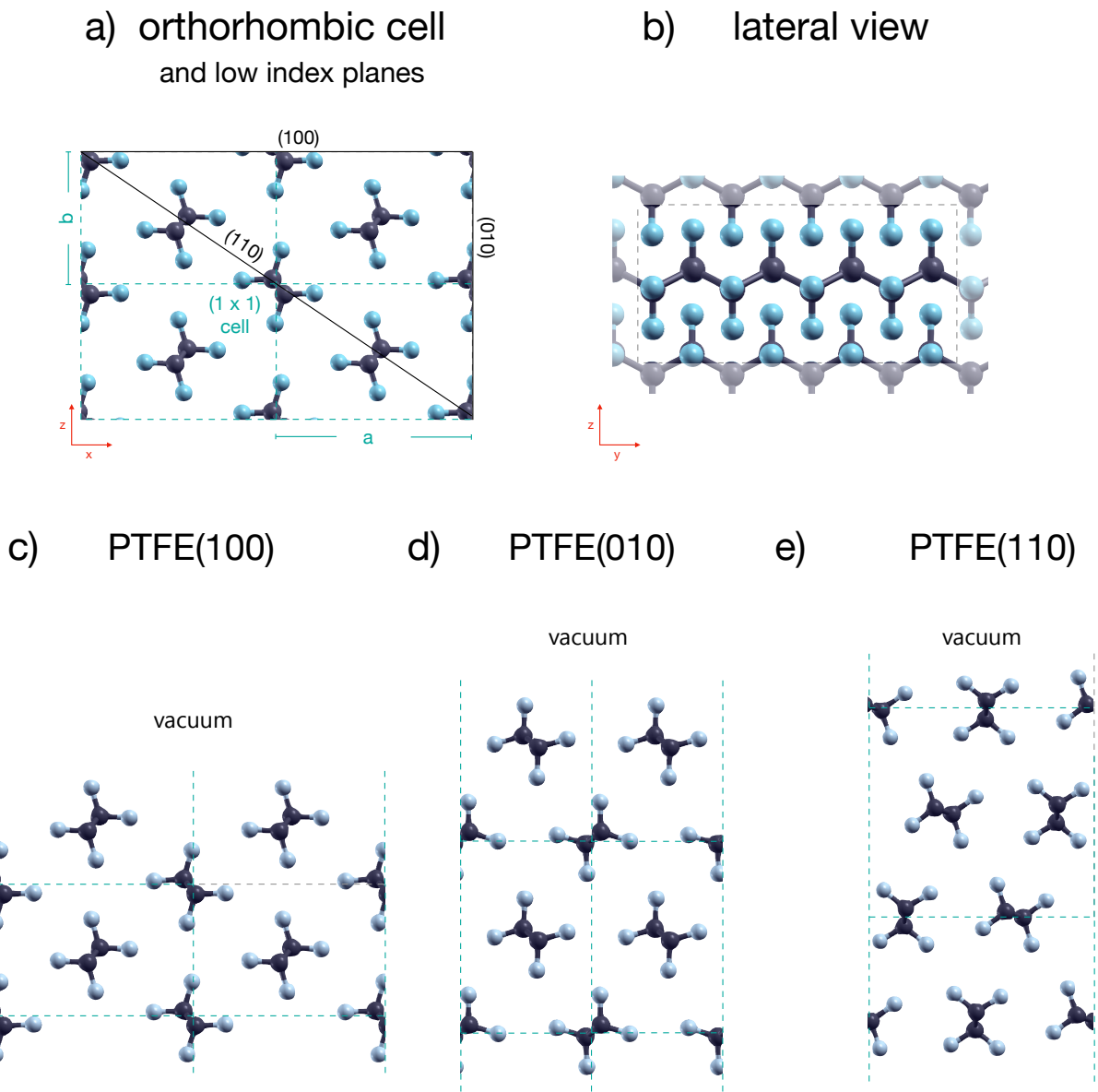$$\rho(z) = \int dxdy\rho^2(x, y, z) \tag{1}$$

4

Figure 1: a) front view of the orthorhombic PTFE lattice. A (2×2) supercell is represented, and the directions of the (100), (010) and (110) planes are highlighted. b) lateral view of the zig-zag chain conformation. In transparency the periodic replicas are shown. c) PTFE(100), d) PTFE(010), e) PTFE(110) surfaces.

The same formula was used to calculate the planar average of the square modulus of the wave functions.

Results and discussion

We started by optimizing the structures of PTFE(100), PTFE(010) PTFE(110) surfaces and the outcome showed that the structure of the three surfaces do not differ much from their bulk structure, as reported in Table 1.

Table 1: Calculated structural properties of PTFE chains in bulk and low-index surfaces. Bulk data were first reported in Ref.[42]

	C-C-C (deg)	F-C-F (deg)	C-C (Å)	C-F (Å)
PTFE bulk	113.8	109.1	1.58	1.36
PTFE(100)	114.0	109.1	1.58	1.36
PTFE(010)	113.9/114.0	109.1	1.58	1.36
PTFE(110)	114.0	109.1/109.2	1.58	1.36

Then, we analyzed the band structure of the three surfaces to observe if surface states were formed. The results are shown in Figure 2.a. It can be seen that the band structures of the three surfaces are almost identical and extremely similar to the band structure of the bulk (see Figure 2 in Ref.[42]), also, the value of the band gap remains unaltered: $\Delta E_{gap} = 5\,\text{eV}$. The calculated gap value is lower when compared to previous Hartree-Fock studies ($\Delta E_{gap} \sim 8\,\text{eV}$)[31] and experimental measurements ($\Delta E_{gap} \sim 10\,\text{eV}$).[44] This underestimation of the band gap by DFT was expected because it is a well-known problem of GGA in the calculation of the insulating band gap[45]. Furthermore, no surface states can be found inside the gap. These results indicate that generating a surface, which implies removing layers of material that influence vdW inter-chain interaction, does not induce any significant variation in the bands dispersion. This means that the band structure is mainly determined by the C-C and the C-F chemical bonds inside the chains. Therefore, cleaving a surface without breaking any chemical bond cannot generate any surface state, contrarily to the PE study,

where surface states were found independently of the exposed surface.[38] In addition, these outcomes show that the electronic properties of the surfaces do not depend on the surface orientation, so we decided to carry on the study only on the PTFE(100) surface.
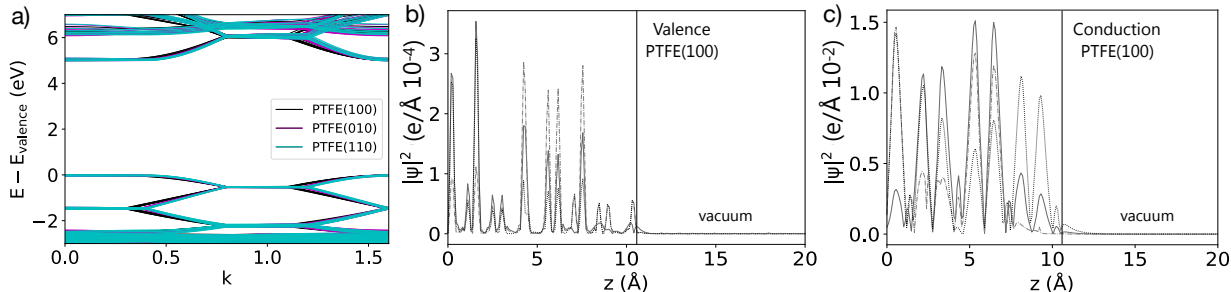

Figure 2: a) Bands structure of PTFE(100) (black), PTFE(010) (magenta) and PTFE(110) (cyan) surfaces. For comparison, band levels are referred to the highest valence band. Plane average of the PTFE(100) b) three highest valence states; c) three lowest conduction states. The surface z position is represented by the vertical line.

By looking at the planar average spatial distribution of the three highest valence states and of the three lowest conduction states[1] it is confirmed that no state is localized on a surface or on specific plane or chain, in fact, they are distributed along the entire slab height (Figure 2b,c).

The absence of surface states inside the band gap means that there is no available state below the conduction band that may act as a deep trap for electrons, thus electron trapping is unlikely. To further understand this conclusion we investigated the surface behavior by either adding or removing one electron.

In the first place, in order to verify the fact that a charge, either negative or positive, added to the slab does not localize on the surface, we calculated the charge density of both the neutral and the charged systems and we computed the planar average by equation 1, to

---

[1]It should be noted that for ultrasoft PP's the squared modulus of the wavefunction is not normalized to 1 by QE.

obtain $\rho(z)$. Then we calculated

$$\Delta\rho_{neg}(z) = \rho_{negative}(z) - \rho_{neutral}(z) \tag{2}$$

$$\Delta\rho_{pos}(z) = \rho_{neutral}(z) - \rho_{positive}(z), \tag{3}$$

where $\Delta\rho_{neg}$ and $\Delta\rho_{pos}$ are the charge density difference between the negatively charged slab (electron added) and the neutral slab and the charge density difference between the neutral slab and the positively charged slab (electron removed), respectively. In this way we can observe the z-dependence of the additional or removed charge and observe where it is localized (or delocalized) within the slab. The calculated charge differences are shown in Figure 3. It can be seen that in both cases the charge difference between the neutral and the charged slabs is distributed along the entire slab height and does not localize on the surface.

In the second place, we studied the relative stability of the charged systems in relation to the neutral slab by calculating the energy differences caused by the addition or the removal of an electron. We considered the ionization potential, $E_I = E_{N-1} - E_N$, and the electron affinity, $E_A = E_N - E_{N+1}$, where N is the number of electrons in the neutral slab. E_I refers to the energy required to remove an electron from the system and it is always positive because removing an electron from a bound state always costs energy. E_A estimates the energy to bind an electron to the system and it can be either positive, if trapping an electron is energetically favorable, or negative, if it is unfavorable. Coherently with the absence of trap states, we found that either when positively or negatively charged the surface becomes less stable: $E_I = 5.33\,\mathrm{eV}$ and $E_A = -0.48\,\mathrm{eV}$. A large ionization potential is to be expected for a large gap insulator like PTFE, while finding a negative electron affinity is more interesting because it indicates that a free electron loses stability when binding to PTFE. This peculiar behavior can be expected by considering that C-F bonds have a strong ionic character due to fluorine high electronegativity and that fluorine atoms have a strong negative charge and they are external in PTFE chains, so it is unlikely for additional electrons to bind to PTFE

chains. It is clear, then, that pristine PTFE surfaces do not offer proper conditions to acquire neither negative nor positive charge.
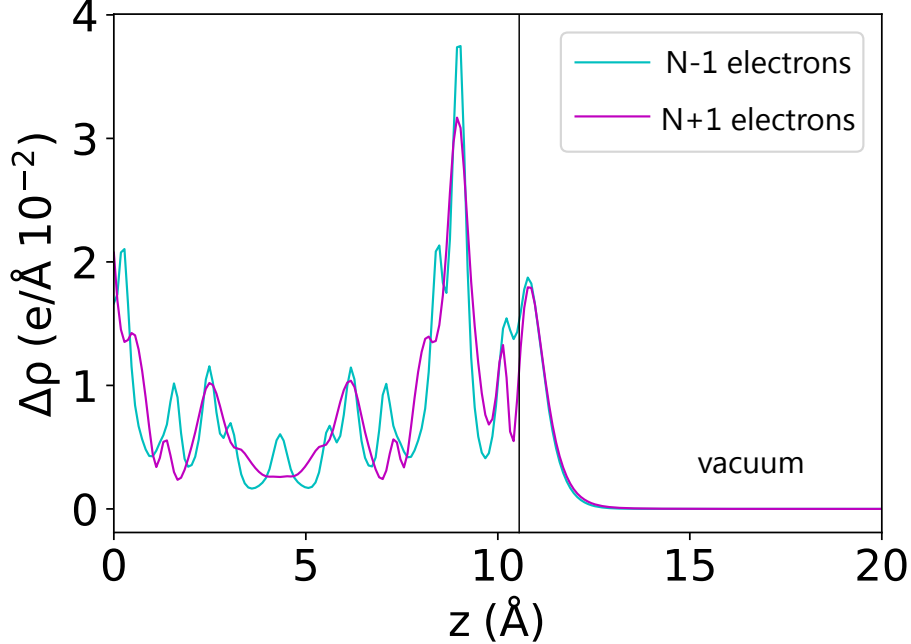

Figure 3: Charge difference between neutral PTFE(100) surface and the same surface with one more electron (cyan line), and with one fewer electron (magenta line).

It follows that some chemical bond cleavage is necessary to modify the electronic properties in order for the surface to be charged. We decided to study the simplest possible defect: we removed one surface fluorine and studied how this removal modifies the structural and electronic properties. The optimized structure is shown in Figure 4. The energy required for the formation of a fluorine vacancy was calculated using the following relation: $E_{def} = E_{surf,def} + E_F - E_{surf}$, where $E_{surf,def}$ is the energy of the defluorinated surface, E_F is the energy of an isolated F and E_{surf} is the energy of the pristine surface. The vacancy formation was found to be energetically costly, around $E_{def} \sim 6\,\text{eV}$. However, it has been experimentally demonstrated that in tribological contact high stresses and temperature flashes provide enough energy to break PTFE chains.[46–48] There is evidence as well that material transfer can drive tribocharging of PTFE.[20] Moreover Molecular Dynamics simulations

have specifically shown that defluorination occurs during sliding contact[46]. Therefore, it is reasonable to assume that such a defect would occur on the surface.

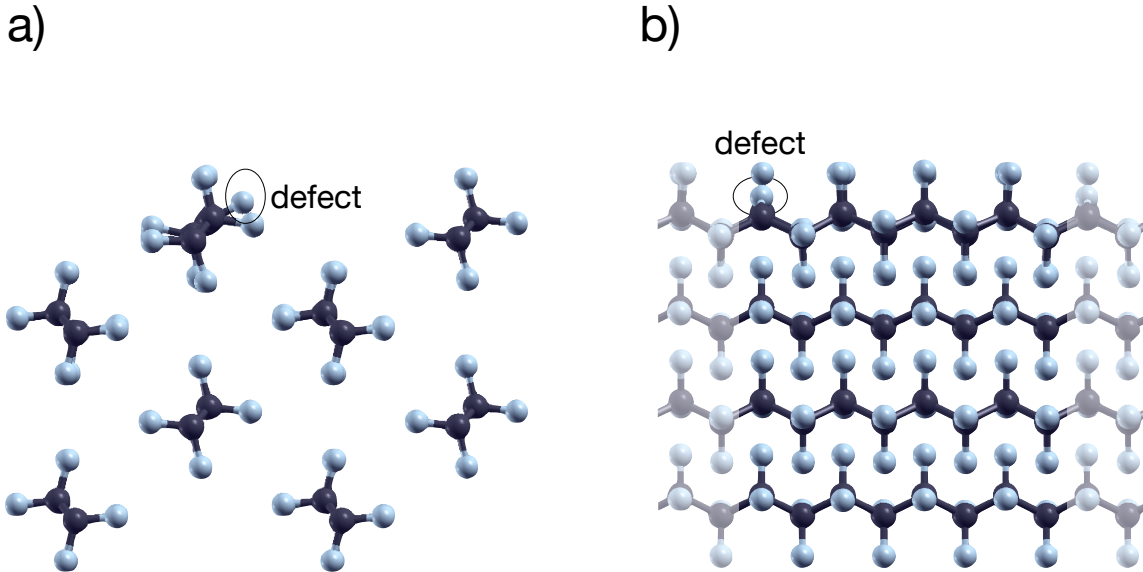a)   b)

Figure 4: a) Front view and b) lateral view of a defective PTFE(100) surface.

The fluorine vacancy induces structural modifications on the involved chain, observable in Figure 4 and reported in Table 2. In particular the C-C-C angle around the defective site is flattened, and consequently the surrounding C-C bonds are shortened from 1.58 Å to 1.52 Å. Also, the remaining C-F bond is rotated from its original position, for symmetry reasons.

Table 2: Calculated structural properties of the PTFE defective chain. In the first are reported row the parameters relative to the chain site where the vacancy is introduced, in the second raw the parameters relative to the nearest neighbor sites, and in the third raw the other sites.

	C-C-C (deg)	F-C-F (deg)	C-C (Å)	C-F (Å)
defect	120.8	—	1.52	1.34
nn	114.7	107.1	1.58	1.37
others	116.1	109.1/109.3	1.59	1.36

The deformations induced by the defect also affect the band structure, comparing Figure 2.a with Figure 5, a little modification of the highest valence states dispersion and the

10

appearance of a defect state inside the band gap can be observed. This state, like the surface states below the conduction band observed in previous study on PE[38], may act as an electron trap because the C electron formerly involved in a C-F bond remains unpaired.

Because it is also possible that the unpaired electron is removed in the fluorine dissociation process, due to F high electronegativity and the ionicity of the C-F bond, we studied the defective slab, both negatively and positively charged.

We calculated again charge difference $\Delta\rho(z)$ (Equation 3) to observe the charge rearrangement with the addition or the removal of an electron. The results are shown in Figure 5.b. When the system is positively charged, we can see that the charge density difference is distributed along the slab but with a large and high concentration at the surface defect location. This effect is much stronger when an electron is added, in fact, a significant charge accumulation can be observed around the defect. The charge peaks and the depletion along the slab can be interpreted as a consequence of the additional electron which forces a charge rearrangement along the entire slab.
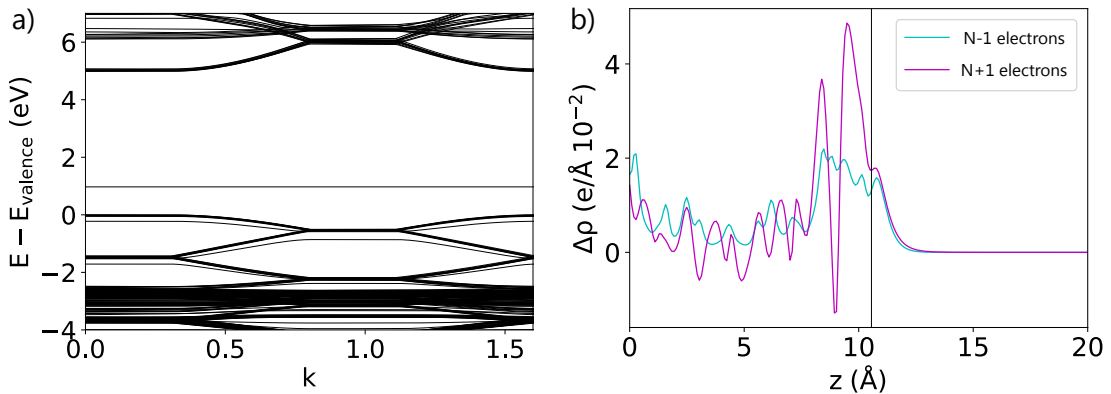

Figure 5: a) Defective PTFE(100) band structure. Band levels are referred to the highest valence band. b) Charge difference between neutral defective surface and the same surface with one more electron (cyan line), and with one fewer electron (magenta line).

This charge rearrangement suggests that for an electron is more convenient to bind to a defective PTFE chain. By calculating the energy difference, we find, indeed, that the system negatively charged is more stable than the neutral: $E_A = 0.47\,\text{eV}$. This means that the

defect affects the electronic properties and favors the acquisition of an additional electron. Conversely, the surface is strongly destabilized by removing an electron: $E_I = 5.27\,\text{eV}$, *i.e.* the ionization potential is reduced by $\sim 1\%$ with respect to the pristine surface, which means that a positively charged configuration is highly unfavorable also in presence of a defect.

Conclusions

In this work we employed an *ab-initio* DFT approach to study for the first time the structural and electronic properties of PTFE low-index surfaces in the high-pressure phase providing insights into the PTFE capability of acquiring and retaining negative charge. We first show that structural and electronic properties of PTFE(100), PTFE(010) and PTFE(110) are similar to the bulk and no surface states or peculiar surface features arise.

Focusing on PTFE(100), we find that, coherently with the absence of surface states, the pristine surface does not possess the suitable properties to acquire negative charge. In fact, adding an electron reduces the system stability. A similar result is found when the surface is positively charged by removing an electron, however, with a much larger energetic destabilization. This demonstrates that, in the absence of any bond rupture and defects, electron transfer is highly unfavorable and, therefore, that it should be preceded at least by ionic transfer for triboelectrification to occur.

By introducing a fluorine vacancy on the surface, we prove that a defect induces the suitable conditions to acquire and retain electronic charge on the surface. An additional electron can stabilize the system by binding to the electron of the carbon atom left unpaired by the defluorination. Contrariwise, a positive charging remains strongly unfavorable also in the defective configuration. The explanation from first principles of the mosaic charge pattern will thus require further investigation of more complex chemistry, involving the rupture of larger polymer fragments and the severing of C-C bonds.

This study provides a first theoretical understanding of PTFE triboelectric behavior and

demonstrates how surface defects play a key role on the PTFE capability of acquiring and retaining negative charge in tribological contact. We provide evidence that, on pristine PTFE surfaces, tribocharging cannot be induced by electrons only. We show that ionic transfer is necessary also for electron transfer and it is one of the processes driving PTFE triboelectrification in its high-pressure phase, the most favorable in tribological conditions. This understanding will prove important for the future development of efficient PTFE-based triboelectric nanogenerators.

Acknowledgement

Supporting Information Available

This will usually read something like: "Experimental procedures and characterization data for all new compounds. The class will automatically add a sentence pointing to the information on-line:

References

(1) Niu, S.; Liu, Y.; Wang, S.; Lin, L.; Zhou, Y. S.; Hu, Y.; Wang, Z. L. Theory of Sliding-Mode Triboelectric Nanogenerators. *Advanced Materials* **2013**, *25*, 6184–6193.

(2) Wang, Z. L. Triboelectric Nanogenerators as New Energy Technology for Self-Powered Systems and as Active Mechanical and Chemical Sensors. *ACS Nano* **2013**, *7*, 9533–9557, PMID: 24079963.

(3) Wang, Z. L. Triboelectric nanogenerators as new energy technology and self-powered sensors: Principles, problems and perspectives. *Faraday Discuss.* **2014**, *176*, 447–458.

(4) Su, Y.; Chen, J.; Wu, Z.; Jiang, Y. Low temperature dependence of triboelectric effect for energy harvesting and self-powered active sensing. *Applied Physics Letters* **2015**, *106*, 013114.

(5) Lacks, D. J.; Sankaran, R. M. Contact electrification of insulating materials. *Journal of Physics D: Applied Physics* **2011**, *44*, 453001.

(6) Lacks, D. J.; Shinbrot, T. Long-standing and unresolved issues in triboelectric charging. *Nature Reviews Chemistry* **2019**, *3*, 465–476.

(7) Lowell, J.; Rose-Innes, A. Contact electrification. *Advances in Physics* **1980**, *29*, 947–1023.

(8) Shen, X.; Wang, A. E.; Sankaran, R. M.; Lacks, D. J. First-principles calculation of contact electrification and validation by experiment. *Journal of Electrostatics* **2016**, *82*, 11 – 16.

(9) Lin, S.-q.; Shao, T.-m. Bipolar charge transfer induced by water: experimental and first-principles studies. *Phys. Chem. Chem. Phys.* **2017**, *19*, 29418–29423.

(10) Xu, C.; Zi, Y.; Wang, A. C.; Zou, H.; Dai, Y.; He, X.; Wang, P.; Wang, Y.-C.; Feng, P.; Li, D.; Wang, Z. L. On the Electron-Transfer Mechanism in the Contact-Electrification Effect. *Advanced Materials* **2018**, *30*, 1706790.

(11) Zhang, Y.; Shao, T. Effect of contact deformation on contact electrification: a first-principles calculation. *Journal of Physics D: Applied Physics* **2013**, *46*, 235304.

(12) Ciniero, A.; Le Rouzic, J.; Reddyhoff, T. The Use of Triboemission Imaging and Charge Measurements to Study DLC Coating Failure. *Coatings* **2017**, *7*, 129.

(13) Ciniero, A.; Rouzic, J. L.; Baikie, I.; Reddyhoff, T. The origins of triboemission – Correlating wear damage with electron emission. *Wear* **2017**, *374-375*, 113 – 119.

(14) Diaz, A. F.; Wollmann, D.; Dreblow, D. Contact electrification: ion transfer to metals and polymers. *Chemistry of Materials* **1991**, *3*, 997–999.

(15) McCarty, L. S.; Winkleman, A.; Whitesides, G. M. Electrostatic Self-Assembly of Polystyrene Microspheres by Using Chemically Directed Contact Electrification. *Angewandte Chemie International Edition* **2007**, *46*, 206–209.

(16) Hogue, M.; Buhler, C.; Calle, C.; Matsuyama, T.; Luo, W.; Groop, E. Insulator-insulator contact charging and its relationship to atmospheric pressure. *Journal of Electrostatics* **2004**, *61*, 259 – 268.

(17) Hogue, M.; Mucciolo, E.; Calle, C.; Buhler, C. Two-phase equilibrium model of insulator-insulator contact charging with electrostatic potential. *Journal of Electrostatics* **2005**, *63*, 179 – 188, Selected Papers from the ESA 2004 Annual Conference.

(18) Salaneck, W. R.; Paton, A.; Clark, D. T. Double mass transfer during polymer-polymer contacts. *Journal of Applied Physics* **1976**, *47*, 144–147.

(19) Baytekin, H. T.; Baytekin, B.; Incorvati, J. T.; Grzybowski, B. A. Material Transfer and Polarity Reversal in Contact Charging. *Angewandte Chemie International Edition* **2012**, *51*, 4843–4847.

(20) Burgo, T. A. L.; Ducati, T. R. D.; Francisco, K. R.; Clinckspoor, K. J.; Galembeck, F.; Galembeck, S. E. Triboelectricity: Macroscopic Charge Patterns Formed by Self-Arraying Ions on Polymer Surfaces. *Langmuir* **2012**, *28*, 7407–7416, PMID: 22530971.

(21) Ciniero, A.; Fatti, G.; Righi, M. C.; Dini, D.; Reddyhoff, T. A Combined Experimental and Theoretical Study on the Mechanisms Behind Tribocharging Phenomenon and the Influence of Triboemission. *Tribology Online* **2019**, *14*, 367–374.

(22) Henniker, J. Triboelectricity in polymers. *Nature* **1962**, *196*, 474–474.

(23) Diaz, A.; Felix-Navarro, R. A semi-quantitative tribo-electric series for polymeric materials: the influence of chemical structure and properties. *Journal of Electrostatics* **2004**, *62*, 277 – 290.

(24) Baytekin, H. T.; Patashinski, A. Z.; Branicki, M.; Baytekin, B.; Soh, S.; Grzybowski, B. A. The Mosaic of Surface Charge in Contact Electrification. *Science* **2011**, *333*, 308–312.

(25) Clark, D.; Kilcast, D. Study of core and valence energy levels of PTFE. *Nature Physical Science* **1971**, *233*, 77–79.

(26) Pireaux, J.; Riga, J.; Caudano, R.; Verbist, J.; Andre, J.; Delhalle, J.; Delhalle, S. Electronic structure of fluoropolymers : Theory and esca measurements. *Journal of Electron Spectroscopy and Related Phenomena* **1974**, *5*, 531 – 550, The International Journal on Theoretical and Experimental Aspects of Electron Spectroscopy.

(27) Delhalle, J. Influence of chemical substitution on energy band structure of polyfluoroethylenes. *Chemical Physics* **1974**, *5*, 306 – 314.

(28) Nakafuku, C.; Takemura, T. Crystal Structure of High Pressure Phase of Polytetrafluoroethylene. *Japanese Journal of Applied Physics* **1975**, *14*, 599–602.

(29) Falk, J. E.; Fleming, R. J. Study of the electronic band structure of polyacetylene and the polyfluoroethylenes. *Journal of Physics C: Solid State Physics* **1975**, *8*, 627–646.

(30) Morokuma, K. Electronic Structures of Linear Polymers. II. Formulation and CNDO/2

Calculation for Polyethylene and Poly(tetrafluoroethylene). *The Journal of Chemical Physics* **1971**, *54*, 962–971.

(31) Kasowski, R. V.; Hsu, W. Y.; Caruthers, E. B. Electronic properties of polyacetylene, polyethylene, and polytetrafluoroethylene. *The Journal of Chemical Physics* **1980**, *72*, 4896–4900.

(32) D'Amore, M.; Talarico, G.; Barone, V. Periodic and High-Temperature Disordered Conformations of Polytetrafluoroethylene Chains: An ab Initio Modeling. *Journal of the American Chemical Society* **2006**, *128*, 1099–1108, PMID: 16433525.

(33) D'Amore, M.; Auriemma, F.; De Rosa, C.; Barone, V. Disordered Chain Conformations of Poly(tetrafluoroethylene) in the High-Temperature Crystalline Form I. *Macromolecules* **2004**, *37*, 9473–9480.

(34) Lorenzen, M.; Hanfland, M.; Mermet, A. Poly(tetrafluoroethylene) under pressure: X-diffraction studies. *Nuclear Instruments and Methods in Physics Research Section B: Beam Interactions with Materials and Atoms* **2003**, *200*, 416 – 420, Proceedings of the E-MRS 2002 Symposium I on Synchrotron Radiation and Materials Science.

(35) Flack, H. D. High-pressure phase of polytetrafluoroethylene. *Journal of Polymer Science Part A-2: Polymer Physics* **1972**, *10*, 1799–1809.

(36) Eby, R.; Clark, E.; Farmer, B.; Piermarini, G.; Block, S. Crystal structure of poly(tetrafluoroethylene) homo- and copolymers in the high pressure phase. *Polymer* **1990**, *31*, 2227 – 2237.

(37) Gosvami, N. N.; Bares, J. A.; Mangolini, F.; Konicek, A. R.; Yablon, D. G.; Carpick, R. W. Mechanisms of antiwear tribofilm growth revealed in situ by single-asperity sliding contacts. *Science* **2015**, *348*, 102–106.

(38) Righi, M. C.; Scandolo, S.; Serra, S.; Iarlori, S.; Tosatti, E.; Santoro, G. Surface States and Negative Electron Affinity in Polyethylene. *Phys. Rev. Lett.* **2001**, *87*, 076802.

(39) Giannozzi, P. et al. QUANTUM ESPRESSO: a modular and open-source software project for quantum simulations of materials. *Journal of Physics: Condensed Matter* **2009**, *21*, 395502.

(40) Perdew, J. P.; Burke, K.; Ernzerhof, M. Generalized Gradient Approximation Made Simple. *Phys. Rev. Lett.* **1996**, *77*, 3865–3868.

(41) Grimme, S. Semiempirical GGA-type density functional constructed with a long-range dispersion correction. *Journal of Computational Chemistry* **2006**, *27*, 1787–1799.

(42) Fatti, G.; Righi, M. C.; Dini, D.; Ciniero, A. First-Principles Insights into the Structural and Electronic Properties of Polytetrafluoroethylene in Its High-Pressure Phase (Form III). *The Journal of Physical Chemistry C* **2019**, *123*, 6250–6255.

(43) Monkhorst, H. J.; Pack, J. D. Special points for Brillouin-zone integrations. *Physical review B* **1976**, *13*, 5188.

(44) Seki, K.; Tanaka, H.; Ohta, T.; Aoki, Y.; Imamura, A.; Fujimoto, H.; Yamamoto, H.; Inokuchi, H. Electronic structure of poly(tetrafluoroethylene) studied by UPS, VUV absorption, and band calculations. *Physica Scripta* **1990**, *41*, 167–171.

(45) Perdew, J. P.; Levy, M. Physical Content of the Exact Kohn-Sham Orbital Energies: Band Gaps and Derivative Discontinuities. *Phys. Rev. Lett.* **1983**, *51*, 1884–1887.

(46) Barry, P. R.; Chiu, P. Y.; Perry, S. S.; Sawyer, W. G.; Phillpot, S. R.; Sinnott, S. B. The effect of normal load on polytetrafluoroethylene tribology. *Journal of Physics: Condensed Matter* **2009**, *21*, 144201.

(47) Harris, K. L.; Pitenis, A. A.; Sawyer, W. G.; Krick, B. A.; Blackman, G. S.;

Kasprzak, D. J.; Junk, C. P. PTFE Tribology and the Role of Mechanochemistry in the Development of Protective Surface Films. *Macromolecules* **2015**, *48*, 3739–3745.

(48) Onodera, T.; Kawasaki, K.; Nakakawaji, T.; Higuchi, Y.; Ozawa, N.; Kurihara, K.; Kubo, M. Effect of Tribochemical Reaction on Transfer-Film Formation by Poly(tetrafluoroethylene). *The Journal of Physical Chemistry C* **2014**, *118*, 11820–11826.

Graphical TOC Entry